# Kinetics of the CO oxidation reaction on Pt(111) studied by in situ high-resolution x-ray photoelectron spectroscopy

M. Kinne, T. Fuhrmann, J. F. Zhu, C. M. Whelan, R. Denecke, and H.-P. Steinrück

Citation: The Journal of Chemical Physics **120**, 7113 (2004); doi: 10.1063/1.1669378
View online: http://dx.doi.org/10.1063/1.1669378
View Table of Contents: http://scitation.aip.org/content/aip/journal/jcp/120/15?ver=pdfcov
Published by the AIP Publishing

# Kinetics of the CO oxidation reaction on Pt(111) studied by *in situ* high-resolution x-ray photoelectron spectroscopy

M. Kinne, T. Fuhrmann, J. F. Zhu, C. M. Whelan,[a] R. Denecke,[b] and H.-P. Steinrück
*Physikalische Chemie II, Universität Erlangen-Nürnberg, Egerlandstr. 3, 91058 Erlangen, Germany*

(Received 18 September 2003; accepted 20 January 2004)

High-resolution x-ray photoelectron spectroscopy has been used to study the kinetics of the CO oxidation reaction on a Pt(111) surface *in situ*. The study focuses on the interaction of a preadsorbed $p(2\times2)$ layer of atomic oxygen with CO dosed using a supersonic molecular beam. Measurements of O 1s and C 1s spectra at 120 K show that CO adsorbs on the oxygen precovered substrate, but no reaction occurs. A maximum CO coverage of 0.23 ML (monolayer) is observed, with CO exclusively bound on on-top sites. In accordance with the literature, bridge sites are blocked by the presence of atomic oxygen. The reaction of CO with preadsorbed O to $CO_2$ is studied isothermally in a temperature range between 275 and 305 K. The reaction rate initially increases with CO pressure, but saturates at $9\times10^{-7}$ mbar. The data indicate that a certain amount of disordered oxygen within the $p(2\times2)$ layer acts as a starting point of the reaction and for a given temperature reacts with a higher rate than O in the well-ordered oxygen $p(2\times2)$ phase. For the reaction of CO with this ordered phase, the results confirm the assumption of a reaction mechanism, which is restricted to the edges of compact oxygen islands. The activation energy of the reaction is determined to $(0.53\pm0.04)$ eV, with a prefactor of $4.7\times10^{6\pm0.7}$ $s^{-1}$. © *2004 American Institute of Physics.* [DOI: 10.1063/1.1669378]

## I. INTRODUCTION

In the field of heterogeneous catalysis the oxidation of carbon monoxide to $CO_2$ on the Pt(111) surface is probably the most extensively studied example of an activated Langmuir–Hinshelwood reaction.[1,2] The common interest in this particular system is on the one hand due to its technological relevance in automotive catalysts; on the other hand, its relative simplicity makes it an ideal model system for the understanding of surface reactions.

The reaction mechanism is known to consist of the following substeps:[2] (1) adsorption of $O_2$ and CO, (2) dissociation of $O_2$ (ad) to 2 O (ad), (3) reaction $CO+O\rightarrow CO_2$, and finally (4) desorption of $CO_2$. In order to investigate the fundamental properties of the reaction step (3) it was found helpful to exclude the influence of the oxygen adsorption and dissociation process by starting out with a surface covered with atomic oxygen, on which CO is dosed subsequently.[3–8] Then the adsorption of CO remains the only additional limiting factor, as the reaction product is known to desorb very rapidly at temperatures above ~270 K at which the reaction takes place.[9]

As a common method to study reaction kinetics, mass spectrometry has been used to detect desorbing $CO_2$. For example, Gland and Kollin[4] found by temperature-programmed reaction experiments activation energies ranging from 1.72 eV for small coverages to 0.70 eV for larger coverages of CO and O. More recently, Zaera and co-workers[5,6] obtained a strongly disagreeing value of 0.39 eV in the limit of low coverages from isothermal molecular beam experiments, but also a strong coverage dependence of the energy. The latter value was obtained with the assumption of a first-order dependence of the rate on the CO and O coverages. In contrast to that, Gland and Kollin[4,10] proposed that the reaction is restricted to the edges of oxygen islands. More recently, this was confirmed by real-time scanning tunneling microscopy (STM) experiments of Wintterlin and co-workers,[7,8] resulting in a reaction order of the atomic oxygen coverage near 0.5. This finding disproves the conclusion from isotopic labeling experiments of Akhter and White[11] that the reaction occurs within the mixed $p(2\times2)$ O–CO coadsorption phase. The geometric structure of the mixed phase has been examined by Bleakley and Hu[12] using density functional theory calculations. Wintterlin and co-workers calculated an activation energy of 0.49 eV, which is found constant with respect to the oxygen partial coverage. However, this experimental approach does not provide information about different adsorption sites and it is limited to rather low temperatures (up to 274 K). Spectroscopic information on the O/CO coadsorbate phase, mainly from high-resolution electron-energy-loss spectroscopy (HREELS)[10,13] and infrared absorption spectroscopy (IRAS),[14] is available from static experiments—i.e., for low temperatures—where no reaction takes place. Agreement is found that CO adsorbs on a saturated atomic oxygen layer only on linearly coordinated (on-top) sites, whereas on the clean Pt(111) surface also twofold-coordinated (bridge) sites are populated.

Despite the thorough research performed so far, the outlined discrepancies in the recent literature indicate that the CO oxidation is still not completely understood and should be examined by new surface science methods. Since the

[a]Present address: IMEC, Kapeldreef 75, B-3001 Leuven, Belgium.
[b]Author to whom correspondence should be addressed. Electronic mail: Reinhard.Denecke@chemie.uni-erlangen.de

availability of third-generation synchrotron radiation the use of *in situ* high-resolution x-ray photoelectron spectroscopy (HR-XPS) has been proven to be a powerful tool in the investigation of surface reactions,[15] as it provides site-specific quantitative information on the adsorbates. In particular, CO oxidation has already been studied on other surfaces—e.g., Rh(110) (Ref. 16) or Pd(110) (Ref. 17)—by this method.

In this paper, time-resolved *in situ* HR-XPS measurements on the coadsorption and reaction of CO with atomic oxygen on Pt(111) are presented. First, the adsorption of CO on a $p(2\times2)$ atomic oxygen structure at low temperature (100–120 K) is examined and compared to results obtained near room temperature (275 and 295 K). The dependence of the reaction rate on the CO gas phase pressure at a temperature of 295 K is the subject of the next section. The reaction order and activation energy are extracted from isothermal reaction measurements in the range between 275 and 305 K for high sample pressure ($1.3\times10^{-6}$ mbar). Different kinetic models for the reaction mechanism are discussed. Finally, results of a temperature-programmed reaction experiment are used to compare with the result of the isothermal measurement.

## II. EXPERIMENT

All experiments were performed at the BESSY II synchrotron radiation facility in Berlin, Germany, in a transportable UHV chamber, which has already been described elsewhere.[18–20] Briefly, it comprises three separate chambers: (1) An *analysis chamber*, equipped with a hemispherical electron energy analyzer (Omicron EA 125 U7 HR); synchrotron radiation from beamlines U49/1-SGM or U49/2-PGM1 enters at an angle of 50° with respect to the analyser lens system in the plane of linear light polarization. (2) In the *molecular beam chamber* a collimated supersonic beam is produced by expanding CO through a 100-$\mu$m-diam Mo nozzle into the first of three successive differential pumping stages. The molecular beam enters the analysis chamber at an angle of 45° with respect to the analyzer lens system; it runs through the focal point of the analyzer in order to allow for *in situ* measurement of adsorption processes. A flag, mounted on a pneumatic feedthrough in the second stage, allows for fast ($<0.1$ s) switching of the beam. The CO (purity 4.7) was further purified by passing the gas line through a cooling trap at $T\sim220$ K in order to remove Ni carbonyls, which can be produced in the stainless-steel supply tube. In this work the nozzle is held at a constant temperature of 303 K; the kinetic energy of the CO molecules is calculated as 0.09 eV ($E_{\mathrm{kin}}=7/2$ kT; see, e.g., Ref. 21 and references therein). (3) Finally, a *preparation chamber* contains low-energy electron diffraction (LEED) optics, an ion gun, and a quadrupole mass spectrometer. The sample holder is mounted on a *xyz* manipulator with rotational feedthrough, which also allows for variation of the polar angle orientation of the sample. Alternatively to the supersonic molecular beam, gas can also be dosed into the analysis and preparation chambers by a conventional dosing system, which in this work was used for oxygen dosing (Messer Griessheim, purity 4.8).

The Pt(111) sample (diameter 10 mm) is spot-welded to Ta wires and can be heated resistively up to 1500 K (for sample cleaning) and cooled by a $LN_2$ cryostat to 95 K. During XPS, the sample is heated radiatively by a filament positioned at the back in order to avoid disturbing magnetic fields caused by resistive heating. The temperature is measured by a K-type thermocouple spot-welded to the edge of the sample. A linear temperature ramp can be applied by a programmable temperature controller (Eurotherm). The sample was cleaned by repeated cycles of $Ar^+$ ion bombardment (1 kV), heating in oxygen ($1.3\times10^{-7}$ mbar, 300–800 K, approximately 2 K/s ramp), and annealing to 1300 K. After the sample was bulk cleaned, carbon contaminants on the surface could be removed efficiently by a single cycle of heating in oxygen and annealing.

XP spectra were collected at photon energies of 380 eV for C 1s and 650 eV for the O 1s region in normal emission geometry. The light incidence angle in that case was 50° with respect to the surface normal. As the oxygen coverage is the main observable for the determination of kinetic properties, mainly O 1s spectra have been taken. For time-resolved measurements, spectra in this region could be collected within a time as short as 5 s per spectrum ($E_{\mathrm{B}}=527-536$ eV) at a resolution of $\sim$250 meV. The reproducibility of binding energy values within this study is $\pm30$ meV; the calibration of the absolute binding energy scale compared to other studies has an uncertainty of typically $\pm150$ meV.

## III. RESULTS AND ANALYSIS

### A. General aspects

In order to examine the properties of the CO oxidation reaction without the influence of the dissociation of oxygen on the sample, all experiments were performed by starting out with a surface precovered with atomic oxygen onto which CO was dosed subsequently. During the reaction, no further oxygen is added to the surface. At a coverage of 0.25 ML (monolayer) (1 ML is defined as one adsorbate atom/molecule per substrate surface atom) atomic oxygen is known to form a $p(2\times2)$ structure[22] where O atoms are adsorbed in threefold fcc hollow sites.[23,24] This structure was prepared by offering a saturation dose of oxygen [here a dose of 20 L ($1\ \mathrm{L}=10^{-6}$ Torr s) was applied] at 120 K and subsequent annealing to 300 K, which results in dissociation and desorption of part of the oxygen.[23] After cooling the sample in vacuum to $\sim$100 K a sharp $p(2\times2)$ LEED structure could be observed, which was checked after each preparation.

The bold lines in Figs. 1(a) and 1(b) show the O 1s XP spectrum of the O-$p(2\times2)$ structure; it consists of a single asymmetric peak at a binding energy of 529.88 eV, in very good agreement with the literature[25] (all binding energy values are derived by fitting the data with model functions—see below). Subsequent dosing of CO at a background pressure of $4.4\times10^{-9}$ mbar and a sample temperature of 100 K leads to the evolution of a second peak located at 532.88 eV [Fig. 1(a)], which shows a slight shift of 0.08 eV towards larger binding energies during uptake. This peak is identified as on-top CO by comparison with spectra of CO on clean Pt(111),[19,20] where a value of 532.80 eV was observed. During CO adsorption, the height of the oxygen-related peak is attenuated by less than 10% (for exact values see below),

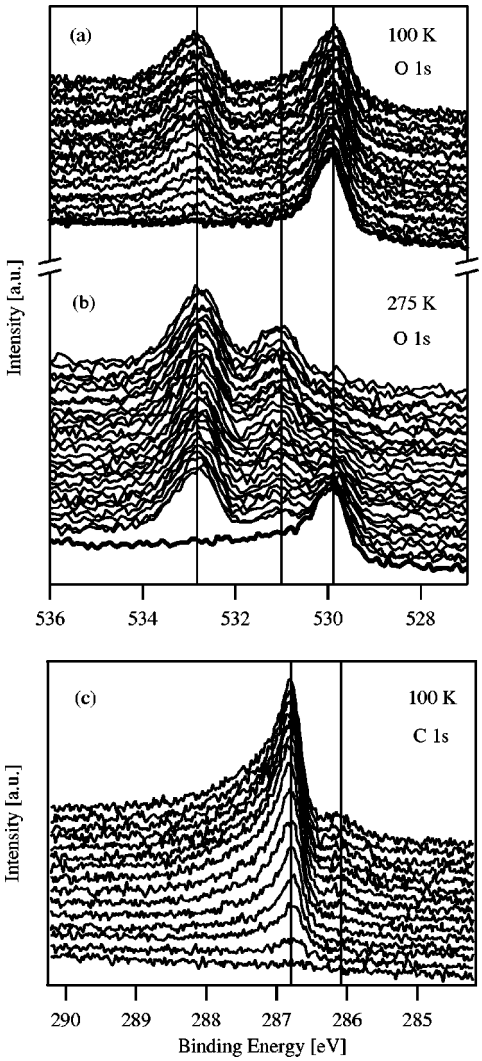


FIG. 1. Normal emission XP spectra during uptake of CO on an O-p(2 $\times$2)-precovered Pt(111) surface. (a) O 1s region, $T=100$ K, $p_{CO}=4.4\times10^{-9}$ mbar, time between spectra: 13 s. (b) O 1s region, $T=275$ K, $p_{CO}=1.3\times10^{-6}$ mbar, time between spectra: 5 s. Bold lines: spectra of pure O-p(2$\times$2) adlayer. (c) C 1s region, $T=100$ K, $p_{CO}=4.4\times10^{-9}$ mbar, time between spectra: 13 s. The gas phase pressure was switched on after the first spectrum in all cases. Excitation energies: $h\nu=650$ eV (O 1s) and 380 eV (C 1s). For binding energy values, see text.

which is in agreement with the reported observation that no reaction takes place.[4,6] No clear peak corresponding to bridge CO is observed, as oxygen is known to block the adsorption of CO on bridge sites.[10] For comparison, the CO uptake at 100 K is also followed by C 1s spectra, which are shown in Fig. 1(c). Like in the O 1s spectra, one CO-related peak evolves at a binding energy of 286.74 eV and shifts towards higher binding energy during uptake. This value is very similar to the value observed for on-top CO on the clean surface.[19,20] At higher exposures, a small second peak at ~286.1 eV is found, corresponding to CO on bridge sites.[19] This small peak amounts to only 0.01–0.02 ML (from quantitative analysis: see below) and was not resolved in the O 1s spectra, as in the latter the corresponding peak is shadowed by the asymmetric signal of atomic oxygen. The occupation of small amounts of bridge sites by CO is attributed to a not completely filled oxygen p(2$\times$2) adlayer. Vacancies in the atomic oxygen layer could be due to the preparation procedure (see above): During heating of the saturated molecular adlayer, oxygen desorbs and, depending on the dissociation and desorption kinetics, vacancies within the remaining ordered atomic oxygen layer can be created. A lower local oxygen coverage could also be present at domain boundaries of the p(2$\times$2) adlayer.

For temperatures of 275 K and above, a reaction is observed, as can be seen from the O 1s spectra in Fig. 1(b): the oxygen peak decreases while a third peak evolves at 530.93 eV, arising from CO adsorbed on bridge sites.[19] During the reaction, again a small change in binding energies of the on-top and bridge CO peaks is observed; the on-top peak shifts from 532.93 eV to lower binding energy by 0.10 eV, while the bridge peak increases its binding energy by about the same value. Peak shifts of that magnitude can be explained by adsorbate–adsorbate interactions, which can be different for the different local surroundings (on-top CO in the mixed CO–O layer and bridge mainly in pure CO regions). The binding energy of the oxygen peak does not show any significant changes. Note that due to the high CO pressure of $1.3\times10^{-6}$ mbar in this case, the on-top CO peak reaches a high intensity immediately after switching on the molecular beam. $CO_2$, which is produced during the reaction, cannot be observed on the sample as it desorbs rapidly at temperatures where the reaction takes place.[22] C 1s spectra during reaction at higher temperatures (spectra not shown) reflect an increase of the bridge related peak at 286.06 eV, similar to O 1s results. The position of this peak is not altered by the presence of oxygen, whereas the on-top species is slightly shifted downwards from 286.76 eV by 0.06 eV.

In order to extract quantitative information and exact peak positions from the raw data, the spectra are fitted with model line shapes. The following procedure is applied to the O 1s spectra: First a straight line fitted to the O 1s region of the clean substrate is subtracted from all spectra, and after that, a Shirley-type[26] background subtraction routine is applied. Then the spectra can be described by a convolution of asymmetric Doniach–Šunjić[27] functions with Gaussians. The shape of the asymmetric atomic oxygen peak is determined from spectra where only this species is present [bottom spectra in Figs. 1(a) and 1(b)]. Spectra where only atomic oxygen and CO on-top species are present [topmost spectrum in Fig. 1(a)] are used to obtain the shape parameters of the on-top CO peak, leading to a symmetric profile. Keeping these parameters fixed, from spectra with a large CO coverage [top spectra in Fig. 1(b)] finally the profile of the CO-bridge contribution is calculated, with a slightly asymmetric shape. Once determined, the same peak shape parameters have been used for all spectra, assuming that the peak shape is not influenced by any coadsorbate interaction. The peak positions are used as fitting parameters, which leads to the above-mentioned binding energies. The C 1s spectra are treated similarly, but here only a linear and no Shirley-background subtraction leads to the best description of the data.[19] In that case both CO peaks are fitted with asymmetric shapes in a similar manner as was done for the O 1s spectra. Peak areas were normalized with respect to the count rate of the clean surface spectrum, such that any decrease in the photon flux

(resulting from a decrease of the storage ring current) is accounted for.

It should be mentioned that in particular for the O 1s spectra the set of parameters describing the different peaks is not unique. One can find different sets of parameters, which would lead to a similar quality of the fit, but would result in different peak areas of the individual species. Furthermore, due to photoelectron diffraction (PED) effects that are not negligible at the low kinetic energies used, the coverages of the various adsorbate species cannot be directly calculated from the peak areas obtained by fitting the XP spectra. Therefore individual calibration factors were determined for the three different species. This calibration was done using structures with known coverage, which are the p(2×2) structure of atomic oxygen ($\theta=0.25$ ML) and the c(4×2) structure of CO ($\theta=0.5$ ML; both bridge and on-top sites are covered with 0.25 ML); the latter can be prepared by dosing 2 L of CO at 200 K and subsequent cooling down to 100 K.[23,28] The ratio of peak areas of on-top and bridge bound species in the O 1s spectra is determined to 1.3 (for $h\nu=650$ eV); this value differs from a ratio of unity, which would have been expected for equal coverages, without PED effects. It agrees qualitatively with the observation of Björneholm *et al.*,[29] although they do not quantify the effect. The intensity of the oxygen peak for the p(2×2) structure also leads to a different scaling factor compared to both CO peaks; the ratio of areas of on-top CO and atomic oxygen peaks is found to be 0.65. For the quantitative analysis the peak areas have been corrected using these calibration factors. In the same way also the peak areas of C 1s spectra have to be weighted with individual scaling factors, the ratio of which (on-top/bridge) has been determined in Ref. 19 has been determined to 1.26 (for $h\nu=380$ eV).

Considering the same quality of fit results for a certain peak shape parameter range and the PED effects, the error bars for the coverages denoted below are difficult to estimate. By testing different fit parameters and considering the reproducibility of the adsorbate structures used for calibration as well as the experimental geometries (e.g., electron emission angle) we estimate the error bars for the absolute coverages given in this paper to ±8%, which corresponds to ±0.02 ML for a coverage of 0.25 ML. One should note that the relative uncertainty within one experimental run (e.g., uptake or isothermal desorption) is smaller. Being aware of these sources of uncertainty, care has been taken that none of the results stated in the following are influenced by experimental artifacts.

### B. Comparison between 120 and 295 K

In the following the results of the quanitative analysis of XP spectra are presented. Figure 2 shows the coverages of the different species present on the surface during the adsorption of CO on the O-p(2×2)-precovered surface, as determined both from O 1s and C 1s spectra. The sample temperatures were 120 K [Fig. 2(a)] and 295 K [Fig. 2(b)] and the pressure in the CO beam was set to $1.3\times10^{-6}$ mbar in both cases (note that for this pressure an exposure time of 1 s corresponds to 1 L).

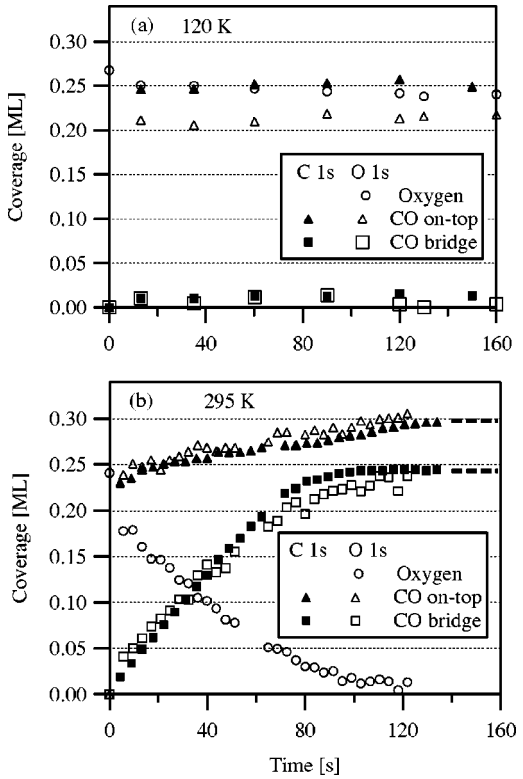


FIG. 2. Coverage vs time for CO uptake on O-p(2×2)/Pt(111) with $p_{CO}=1.3\times10^{-6}$ mbar. CO pressure is switched on at $t=0$. (a) $T=120$ K; solid symbols from C 1s, open symbols from O 1s spectra. (b) $T=295$ K; solid symbols: C 1s, open symbols: O 1s. Bold dashed lines: result after uptake on clean sample under equal conditions.

The results of O 1s and C 1s measurements at 120 K are shown in Fig. 2(a). Immediately after opening the CO beam at $t=0$, the O 1s data (open symbols) show a small decrease of the oxygen coverage by about 0.02 ML. After that, no significant change in the oxygen signal occurs up to a total CO dosing time of 160 s (=160 L). The initial loss in the oxygen signal is interpreted as a damping or a photoelectron diffraction effect caused by neighboring CO molecules. A reaction as an alternative explanation for the decrease in the oxygen signal seems to be unlikely at a temperature of 120 K; no evidence for an effect like that can be found in the literature.[6,14] After the start of the CO exposure, the coverage of the on-top CO species immediately jumps to 0.21 ML and does not increase any further after applying higher doses of CO. Note that the high sample pressure is the reason that saturation of the CO on-top coverage had already been reached before the first spectrum was measured. As already evident from the raw spectra in Fig. 1(a), the contribution of bridge-coordinated CO is almost negligible (0.01–0.02 ML) during the whole uptake. The quantitative analysis of the corresponding C 1s spectra yields very similar results [solid symbols in Fig. 2(a)]: Upon the start of adsorption, the on-top CO coverage immediately builds up, whereas the bridge site occupation is almost negligible (0.01 ML). Like in the O 1s spectra, no further change is observed both in bridge and on-top site occupation at higher exposures. The absolute value of the on-top site occupation is determined to 0.25 ML, which is somewhat larger than obtained from the O 1s measurements, but within the margins of error mentioned above.

By averaging the two values we obtain a saturation coverage of CO on the O-p(2×2) layer of 0.23 ML. This value is in very good agreement with the value of 0.25 ML one would expect for a coadsorbate structure, where each O-p(2×2) unit cell contains one on-top CO molecule, as suggested, e.g., in Ref. 8. It is obtained on the surface immediately after opening the CO beam and no further increase of the CO coverage up to an exposure of 160 L was observed in the present study. This behavior is different compared to CO adsorption on a clean Pt(111) surface, where at the same temperature on-top coverages significantly above 0.25 ML are observed at comparable exposures.[19] It will be shown below that for oxygen coverages below 0.25 ML during the reaction also an increase of CO on-top species to coverages larger than 0.25 ML can be found. Obviously, oxygen atoms not only block bridge sites for CO adsorption, but also a part of the on-top sites available in the absence of O.

The finding of a maximum CO coverage of 0.23 ML on the O-p(2×2) layer is in contrast to the results from temperature-programmed desorption (TPD) experiments by Kostov *et al.*,[13] where after a dose of 100 L at 120 K a CO coverage of 0.41 ML was obtained. Similar observations of a higher CO saturation coverage are reported by Zaera and co-workers,[5,6] with values ranging up to 0.4 ML in the presence of the O-p(2×2) layer. These differences are too large to be explained by damping or diffraction effects of photoelectrons of the coadsorbed CO. A reason for a discrepancy could be different preparation procedures of the O-p(2×2) structure: In the cited contributions[6,13] the O-p(2×2) layer was prepared by applying high exposures of oxygen at temperatures above the dissociation temperature of $O_2$ on Pt(111) which could lead to a different domain structure compared to our experiments. However, both preparation methods yield a sharp p(2×2) LEED pattern. Uncertainties in the calibration procedures could be another possible source of error.

In Fig. 2(b) the results of O 1s (open symbols) and C 1s (solid symbols) measurements at 295 K are shown—i.e., at a temperature at which a reaction between O and CO occurs. Within the margin of error, the CO coverages obtained from the two data sets are in very good agreement with each other. Overall, a steady decrease of the oxygen coverage is observed that is accompanied by a very fast increase in CO on-top coverage, similar to the situation at 120 K, and a much slower increase of the CO bridge coverage. A closer look at the data shows that there is a sudden drop of the oxygen signal (by ~0.05 ML) from its starting value to the first data point after $t=0$, followed by a smoothly declining curve. This effect is always observed in our experiments between 275 and 305 K, with the magnitude of the drop varying between 0.03 and 0.06 ML. An inverse behavior is observed for the CO population on bridge sites: after the molecular beam has been switched on, the signal suddenly rises and thereafter increases smoothly with a slope comparable to the negative slope of the oxygen curve. The quantity of this initial rise is comparable with the drop of the oxygen coverage: i.e., it lies between 0.03 and 0.06 ML. The sudden and opposite intensity changes of the O and CO bridge signals indicate the existence of a fast reaction channel for CO oxidation. This channel could be due to a certain amount of disordered oxygen, which might be present on the surface even though a sharp LEED pattern has been observed, e.g., at the boundaries of ordered p(2×2) domains. As this amount might vary slightly from one preparation of the oxygen layer to another, the mentioned differences for different runs are not surprising. Such a reaction between CO and disordered oxygen was found by Yoshinobu and Kawai[14] in TPD measurements already at a temperature of ~225 K. At $T=295$ K, one would expect that this reaction is very fast and thus could cause the rapid change at the beginning of the CO uptake in our data. After the disordered oxygen species have reacted to $CO_2$, only ordered p(2×2) domains of oxygen coadsorbed with CO should be present on the surface. The reaction of CO with these islands then occurs with a lower reaction rate, which gives rise to the observed slow decrease of the O coverage and increase of CO bridge coverage. In other words, the disordered parts in the oxygen layer act as a starting point of the reaction, which then continues at the edges of compact oxygen islands, as will be outlined below.

From Fig. 2(b) it becomes evident that also the evolution of the CO on-top species at higher temperatures (295 K) is different as compared to low temperatures [120 K, Fig. 2(a)]: After the immediate fast increase of the coverage from zero to ~0.24 ML at the first data point after the start of adsorption a slow, but significant increase up to 0.30 ML at ~120 L is observed. This behavior is similar to the adsorption of CO on the clean Pt(111) surface: There, for total coverages above 0.5 ML, the CO on-top population increases slowly from 0.25 ML to ~0.30 ML for equal experimental conditions, whereas the bridge site occupation of CO stays almost constant at 0.25 ML.[19,20,29] The fact that the slow increase of on-top CO in Fig. 2(b) goes along with the decrease of atomic O again suggests that oxygen atoms partially block the on-top adsorption of CO. For comparison, we have indicated the CO bridge and on-top coverages after exposure onto the clean Pt(111) surface under the same conditions as used here as dashed lines at the right margin of Fig. 2(b). As expected, these values coincide with the corresponding coverages after the reaction ($t=120$ s), where no oxygen is left on the surface.

### C. Pressure dependence of the reaction rate

To simplify the determination of the rate constant of CO oxidation from our experiments it is helpful to exclude the influence of other rate limiting factors, such as the flux of the incoming CO molecules or diffusion processes on a not fully occupied surface. To rule out these effects, a CO pressure should be used, where the impingement rate of CO is much higher than the reaction rate, as has been done in the above experiments. As a consequence, one would expect that bridge sites and additional on-top sites, which after the removal of oxygen become available for CO adsorption, are immediately filled and the CO surface population is saturated. Thus the total speed of the reaction, which is a function of the CO coverage, should reach a saturation value for high pressures. In the following, both the saturation of the CO surface population as well as the reaction rate are

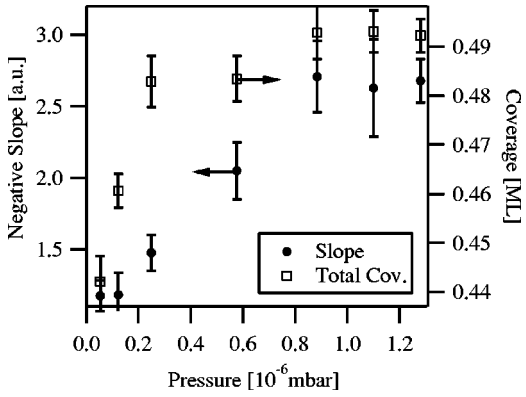


FIG. 3. Reaction rate as determined from the negative average slope of the oxygen coverage for 0.05 ML$<\theta_O<$0.15 ML during reaction ($T=295$ K) vs CO beam pressure (solid circles, left axis). Average total coverage (CO $+$O) for 0.05 ML$<\theta_O<$0.15 ML in the same experiment (open squares, right axis).

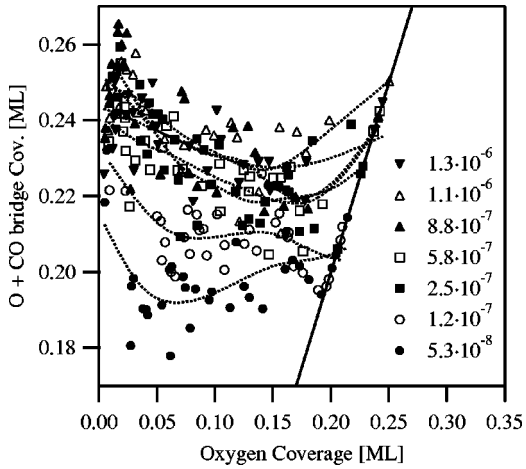


FIG. 4. Sum of the atomic oxygen and bridge CO coverage vs atomic oxygen coverage during reaction at 295 K for different CO pressures. Dotted lines: interpolating splines, as guides to the eye. The solid line indicates the bisector of the graph; the scale of the left axis does not start at zero and therefore the bisecting line does not run through the lower left corner of the graph.

checked for a sample temperature of 295 K and different molecular beam pressures by the same type of experiment as described above [Fig. 2(b)], starting out with an O-p$(2\times2)$ layer.

As a measure of the reaction rate, the slope of the oxygen signal between 0.05 and 0.15 ML is displayed in Fig. 3 as a function of the gas phase pressure (solid circles, left axis). Clearly, a saturation effect is observed for pressures above $\sim9\times10^{-7}$ mbar, indicating that the pressure accessible by the molecular beam is indeed high enough that the reaction rate is not limited by the adsorption of CO. Note that even for the lowest pressure the impingement rate of CO would nominally exceed the reaction rate. In the limit of zero pressure the reaction rate must go to zero.

To check the saturation of the CO population with increasing pressure, we investigate the behavior of the CO bridge$+$O coverage as well as the total CO$+$O coverage. Both values should saturate for a sufficiently high pressure. On the other hand, at lower pressures, for which the impingement rate becomes comparable with the reaction rate, not all vacant sites can be immediately populated by CO and these coverages should drop after the start of the reaction. In Fig. 3, the averaged total CO$+$O population between 0.05 ML$<\theta_O<$0.15 ML (with $\theta_O$ being the atomic oxygen coverage) is included as open circles. The data clearly show the saturation effect starting at a pressure of $2.5\times10^{-7}$ mbar, which is significantly lower than for the reaction speed (see above). Within the margin of error an identical behavior is encountered if the sum of bridge-CO and oxygen is analyzed (data not separately shown in Fig. 3). In Fig. 4 the corresponding data are shown as a function of oxygen coverage for the different pressures. Note that for clarity of the presentation the scale of the left axis in the graph is expanded and does not start at zero coverage and, therefore, the bisecting line does not run through the lower left corner of the graph. Clearly, the data for low pressures (open and solid circles) lie below the data for pressures at and above $2.5\times10^{-7}$ mbar, which are identical within the scatter of $\pm0.01$ ML. Furthermore, for high pressures the sum shows only small deviations [$(0.025\pm0.01)$ ML at $\theta_O=0.10-0.15$ ML] from a constant value of 0.25 ML, which is expected if one oxygen atom blocks the adsorption on one bridge site and free sites are efficiently filled by CO. The reason for the smaller value is most likely that at the edges of the islands not every O can be replaced by CO molecules, which is expected to be most relevant for intermediate O coverages, as is observed. Concerning the low-pressure experiments, at the beginning of the reaction (i.e., for high oxygen coverage) the data points coincide with the bisector of the graph (solid line in Fig. 4), which means that at first almost no CO is found on bridge sites. Later, the data points diverge from the bisector and finally come near the value of 0.25 ML at the end of the reaction (i.e., for zero oxygen coverage), as expected.

Figure 3 shows that saturation of CO coverage and reaction rate occur at different pressures—i.e., $2.5\times10^{-7}$ and $9\times10^{-7}$ mbar, respectively. The reason for this difference could be a repulsive interaction of oxygen and CO, as proposed by Völkening and Wintterlin:[8] Since sites in the vicinity of oxygen atoms are the reactive ones, but simultaneously are energetically unfavorable for the adsorption of CO, the surface can be almost saturated with CO and still a considerable part of the reactive sites would be vacant. This is especially true if the number of reactive sites is small compared to the number of unreactive adsorption sites for CO as would be the case if the reaction were to occur only at the edges of large oxygen islands. As small differences ($\leqslant$0.01 ML) in occupation are not detectable in XPS, it might appear as if the surface is already saturated at a certain pressure, while the reaction speed still increases with pressure.

### D. Temperature dependence of the reaction rate

In order to determine the kinetic parameters of the CO oxidation, isothermal reaction experiments have been performed for different temperatures between 275 and 305 K, using a CO pressure of $1.3\times10^{-6}$ mbar. The experimental values of the oxygen coverage are displayed in Fig. 5 as a

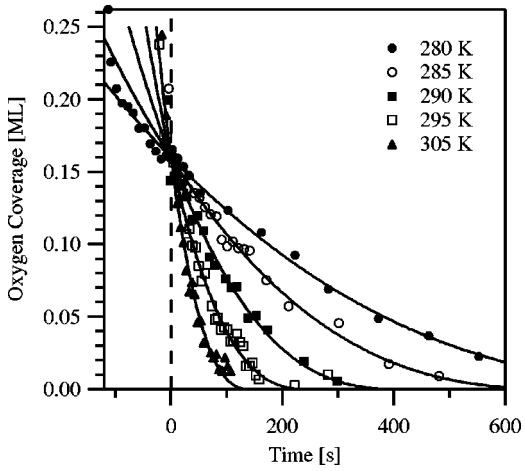


FIG. 5. Coverage of atomic oxygen vs time during reaction for different temperatures. $p_{CO}=1.3\times10^{-6}$ mbar in all cases. Solid lines: fits of the function given in Eq. (6). The time axis has been shifted so that the fit curves coincide in the point ($t=0,\theta_O=0.16$ ML) (see text).

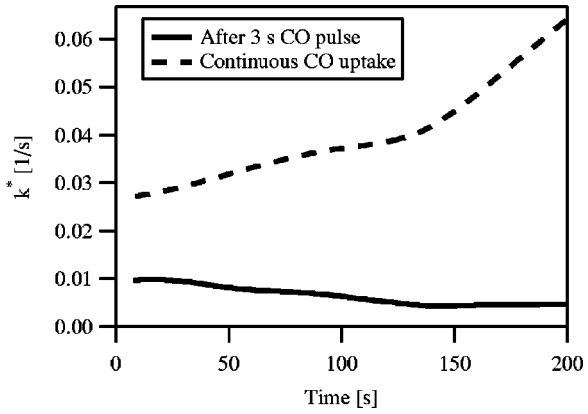


FIG. 6. Ratio $k^*=\dot{\theta}_O/(\theta_O\theta_{CO})$ as a function of time during reaction at $T=300$ K. Dashed line: CO beam ($p_{CO}=1.3\times10^{-6}$ mbar) impinging on the sample during the whole reaction. Solid line: only a short (3 s) CO pulse ($p_{CO}=2\times10^{-6}$ mbar) is applied at the beginning. $\dot{\theta}_O$ has been calculated after smoothing the data curves by spline functions.

function of time. In the graph, the time scale for each experiment is shifted by an offset value, such that at $t=0$ all curves coincide in the point $\theta_O=0.16$ ML, which was done for clarity of presentation because of the following reason: The first data points in each run show that despite equal preparation procedures of the p$(2\times2)$ atomic oxygen layer the observed coverages exhibit some variation. Additionally, since the initial drop of the oxygen coverage also differs slightly from one experiment to another (see Sec. III B), the starting point of the smoothly decreasing part of the reaction curve differs between the experiments, but in any case is found for coverages larger than 0.16 ML. Therefore, taking 0.16 ML as the starting coverage ensures that the initial reaction of disordered oxygen does not affect the following results.

For quantitative analysis of the data in Fig. 5 an appropriate rate equation has to be found, which in the most general case for a Langmuir–Hinshelwood reaction[30] is of the form

$$d\theta_O/dt=-kf(\theta_O,\theta_{CO}), \tag{1}$$

where $\theta_O$ and $\theta_{CO}$ are the coverages of atomic oxygen and CO, respectively, and $k$ is the reaction rate constant. The function $f$ not only depends on the given coverages, but also on the local arrangement of the adsorbates on the surface. A straightforward choice of $f$ is a simple first-order dependence on $\theta_O$ and $\theta_{CO}$, assuming an isotropic distribution of molecules[7]—i.e.,

$$d\theta_O/dt=-k^*\theta_O\theta_{CO}. \tag{2}$$

By calculating the ratio $\dot{\theta}_O/\theta_O\theta_{CO}$, the value of $k^*$ can be obtained during the whole reaction. To do that the derivative $\dot{\theta}_O$ has to be calculated numerically, which due to statistical noise is only possible after smoothing the data curves with interpolating spline functions. If $k^*$ is assumed to be independent of the coverages, Eq. (2) should hold for different surface coverages during the reaction—i.e., for different CO pressures. In order to check this, two extreme cases are compared: an experiment with a CO pressure of $1.3\times10^{-6}$ mbar present during the whole reaction and another one where the O-p$(2\times2)$-covered sample is exposed only to a short, intense pulse (duration 3 s, $p=2.0\times10^{-6}$ mbar) of CO at the beginning. The ratio $\dot{\theta}/\theta_O\theta_{CO}$ for both choices is presented in Fig. 6 as a function of time, clearly showing that the values in the case of the pulse experiment are lower by a factor of 3–13 compared to steady CO exposure. Obviously, $k^*$ is not a constant if it is determined in that way; it varies also significantly within the high-pressure experiment, as was already pointed out by Wintterlin *et al.*[7] One interpretation could be that $k^*$ is strongly coverage dependent, as was suggested by Zaera *et al.*[6] Alternatively, the simple assumption of an isotropic distribution of adsorbates could be wrong. In the last section we could show that the existence of oxygen islands could explain the pressure dependence of the reaction speed if the reaction is restricted to the island edges. The latter assumption also provides a simple explanation for the difference in speed between the measurements in Fig. 6: As it is known that CO can adsorb inside the O-p$(2\times2)$ structure, the possibility of a reaction within this structure would be in contradiction with the observed slow reaction rate after the CO pulse. Within this model Eq. (1) can be written as

$$d\theta_O/dt=-kc\,\theta_O^{\alpha}g(\theta_{CO}), \tag{3}$$

where $c\,\theta_O^{\alpha}=\theta_{O,edge}$ is the number of oxygen atoms at island edges per substrate atom, with $\alpha=0.5$ for smooth (nonfractal) edges and $g$ a still unknown function depending on $\theta_{CO}$. In the simple case where all oxygen islands have the same size, $\theta_{O,edge}$ is given by

$$\theta_{O,edge}=az\sqrt{N_O/z}/N_m=a\sqrt{zN_O}/N_m,$$

where $N_m$ is the number of substrate atoms, $z$ the total number of islands, and $N_O$ the total number of oxygen atoms. $a$ depends on the shape of the islands; in the case of circular islands, $a=2\sqrt{\pi}$. Setting $N_O=\theta_O N_m$, this yields

$$\theta_{O,edge}=a\sqrt{z\,\theta_O}/\sqrt{N_m}$$

and leads by comparison finally to

$$c = a\sqrt{z/N_m}. \tag{4}$$

This means in other words that without knowledge of the island size and shape it is only possible to determine the product $k' = kc$ from our measurement. The function $g(\theta_{CO})$ in Eq. (3) accounts for the density of CO molecules on reactive sites—i.e., at the edge of oxygen islands. In the most general case it depends on the reaction rate, the incoming flux of CO particles, the diffusion constant of adsorbates, and interaction energies between adsorbates. Fortunately, in the high-pressure limit it becomes greatly simplified: then all reactive sites are always fully populated and $g$ reduces to unity. In the last paragraph we could show that this limit is fulfilled in our experiments. Finally, the equation

$$d\theta_O/dt = -k'\theta_O^{\alpha} \tag{5}$$

would be suitable to evaluate our isothermal reaction data, but would involve numerical calculation of the derivative and smoothing of the data curves, as mentioned above. Therefore, it seems better to use the integral form of Eq. (5)—that is,

$$\theta_O = [\theta_O|_{t=t_0}^{1-\alpha} - (1-\alpha)k'(t-t_0)]^{1/(1-\alpha)}, \tag{6}$$

which can be fitted to the curves in Fig. 6(a). As mentioned above, $\theta_O|_{t=t_0}$ is chosen to be 0.16 ML and $t_0$ is the time at which this coverage is observed. Data points near the sudden initial decrease of the oxygen signal are thereby neglected in the following analysis.

In order to check if the assumption of compact islands—i.e., $\alpha = 0.5$—can be justified, first a fit of Eq. (6) with three variable parameters—namely, $\alpha$, $k'$, and $t_0$—is performed, yielding a mean value of

$$\alpha = 0.63 \pm 0.15.$$

Within the given statistical error margin this result is consistent with the hypothesis of a one-dimensional reaction front. The large uncertainty indicates that the shape of the curve shows a relatively weak dependence on $\alpha$. This value is comparable with the one of 0.55 given by Völkening and Wintterlin[8] obtained from STM observations. In a second fit procedure $\alpha$ is held fixed at 0.63 and $k'$ and $t_0$ are determined again, resulting in the curves displayed in Fig. 5 together with the data points. Note that on the time axis ($t - t_0$) rather than $t$ is used, causing all curves to coincide in the point ($t = 0, \theta_O = 0.16$ ML). Now $k'$ can be used to extract the activation energy $E_a$ of the reaction by assuming an Arrhenius-type behavior of the reaction rate—i.e.,

$$k' = c\nu \exp(-E_a/k_B T), \tag{7}$$

where $\nu$ is the preexponential factor and $c$ the parameter defined in Eq. (4). Figure 7 shows $k'$ as a function of the inverse temperature as well as a fit according to Eq. (7), which results in the parameters

$$E_a = (0.53 \pm 0.04)\ \text{eV},$$

$$c\nu = 4.7 \times 10^{6 \pm 0.7}\ \text{s}^{-1}.$$

Using a fixed value of $\alpha = 0.5$ for the fit yields results that are within the given error bars (0.52 eV, $2.4 \times 10^6$ s$^{-1}$).

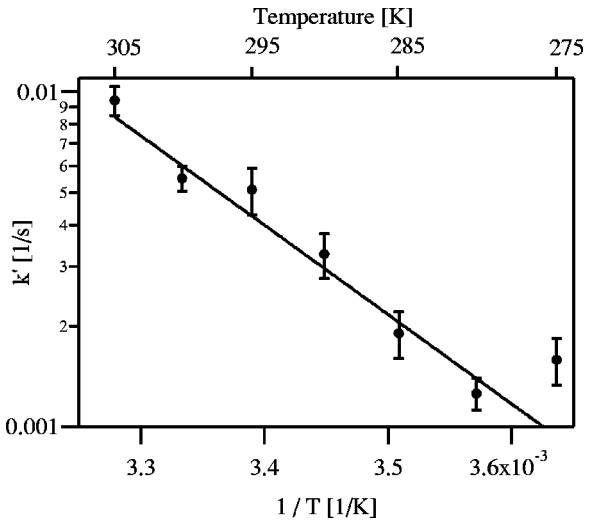


FIG. 7. Arrhenius plot of $k'$ as determined from the fits in Fig. 5 vs inverse temperature. Solid line: exponential fit.

At this point the error bars of these numbers have to be discussed. When comparing the reaction rates for 295 K in Figs. 2(b) and 5, one finds a difference of a factor of 2 in these rates. There are two possible reasons for this difference. It can be attributed to an incorrect calibration of the temperature scale due to a bad connection of the thermocouple to the sample: All data in Figs. 2, 3, 4, and 8 were collected in one experimental period, whereas Figs. 5 and 6 are taken from another period. Between both periods the sample and thermocouples had been remounted. If the temperature deviation were 10 K, the data of the two periods would be in very good agreement with each other. A second source of the observed difference could be a different number of oxygen islands, $z$, due to different surface quality. According to Eq. (4), $c$ is proportional to $z^{1/2}$ and thus a change in the number of oxygen islands by a factor of 4 would lead to a difference in the reaction rate by a factor of 2, as is observed. These uncertainties, either in the temperature measurements or in sample preparation, contribute to the error bars given above.

As $c$ is not known ($c \ll 1$ for extended islands), in any case $\nu$ alone cannot be determined. From the STM work of Völkening and Wintterlin [Fig. 1(a) of Ref. 8] we can estimate that $c$ is of the order of 0.05, so by simply taking the slope of the Arrhenius plot one would underestimate $\nu$ by a factor of ~20. In this STM study[8] an activation energy of 0.49 V and a prefactor of $1.6 \times 10^7$ s$^{-1}$ are obtained in a temperature region from 237 to 274 K, in good agreement with our observation. Within their quoted uncertainty, Zaera *et al.*[6] found comparable values of $E_a = 0.39$ eV and $\nu = 2.5 \times 10^5$ s$^{-1}$ in the limit of zero coverage from their molecular beam study in the range of 300–400 K. In this case, however, an incorrect assumption of an isotropic distribution of adsorbates has been used to model the coverage-dependent data. From a theoretical point of view, Eichler[31] obtained from density functional theory calculations an activation energy of 0.74 eV and a preexponential factor of $5 \times 10^{12}$ s$^{-1}$, values which differ substantially from our and other experimental data. The very high prefactor leads to the

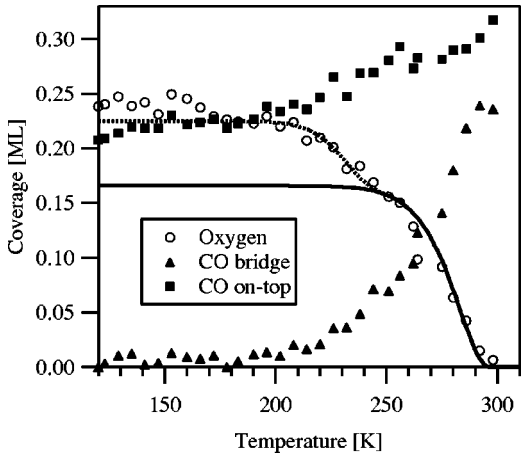


FIG. 8. Coverages of CO and oxygen from O 1s data during temperature-programmed reaction (symbols). CO pressure was set to $1.3\times10^{-6}$ mbar during the whole experiment; a heating rate of 0.1 K/s was applied, starting at 120 K. Lines: calculations without (solid line) and with (dotted line) contribution of disordered oxygen (see text for details).

prediction of a reaction rate which is higher than the experimentally observed one.

### E. Temperature-programmed reaction

To obtain further insight into the process of CO oxidation, we performed a temperature-programmed reaction experiment: The O-p$(2\times2)$-precovered sample is cooled to 120 K and is exposed to $1.3\times10^{-6}$ mbar CO from the molecular beam. After 120 s, the sample temperature is increased linearly with a heating rate of 0.1 K/s, while O 1s spectra are taken approximately every 6 K. The CO impingement rate was the same during the whole experiment. The resulting O and CO coverages are presented in Fig. 8. Up to 200 K only a slow decline of the oxygen signal of about 0.02 ML is observed, while the amount of on-top CO increases approximately by the same amount. As a thermally activated reaction seems unlikely for that temperature, photon-stimulated reaction or desorption could serve as an interpretation. Vacant sites are effectively filled by CO molecules due to the high CO pressure. Above 200 K a steeper decrease of $\theta_O$ follows, with a simultaneous increase of CO on on-top and bridge sites. This effect cannot be explained by the kinetic parameters of the reaction at oxygen islands that have been derived in Sec. III D: at the given time scale they would predict a negligible reaction rate below ~250 K. However, it fits to the fast reaction channel at the start of isothermal experiments discussed in Sec. III C (between 275 and 305 K), which has been explained by a reaction of CO with disordered oxygen atoms. The amount of oxygen involved in this reaction was determined to be 0.03–0.06 ML, which is in agreement with the decrease of $\theta_O$ by 0.05 ML between 200 and 250 K in the temperature-programmed reaction in Fig. 8. Assuming that the reaction of disordered oxygen occurs within that temperature window, it seems plausible, that at 275 K and above this effect would happen faster than the temporal resolution of our XPS measurement.

In order to compare the temperature-programmed experiment with the isothermal reaction, Eq. (5) together with Eq. (7) can be used to calculate the change of oxygen coverage during the temperature increase. Instead of a constant temperature, a linear behavior $T(t)=T_0+\beta t$ (with $\beta$ being the heating rate and $T_0$ the starting temperature) is used and Eq. (5) is solved numerically. With a starting coverage of 0.17 ML, corresponding to the coverage of ordered oxygen regions, one observes a function which is shifted upwards by 10 K as compared to the data points. This discrepancy can easily be explained by either the above-mentioned uncertainty in the temperature scale (Figs. 5 and 8 stem from different measurement periods) or by different surface quality resulting in reaction rates different by a factor of 2. If the simulated curve is shifted down by 10 K, one obtains the solid line in Fig. 8, which above 250 K fits the data points very well.

To also describe the behavior below 250 K, rate equation (5) can be extended by a term, which accounts for the reaction in disordered regions. Thereby one assumes that the oxygen coverage in ordered and disordered regions can be treated independently. The ordered part is still described by Eq. (5), whereas the coverage of disordered oxygen, $\theta_O^d$, can be modeled by

$$d\theta_O^d/dt = -\nu^d \exp(-E_a^d/k_BT)\,\theta_O^d, \tag{8}$$

where $E_a^d$ and $\nu^d$ are the activation energy and prefactor corresponding to disordered oxygen. This first-order dependence on $\theta_O^d$ assumes that all oxygen atoms in the disordered areas are reactive and are surrounded by CO molecules as reaction partners. Note that with the present data basis this assumption is somehow arbitrary, but is the simplest choice which still can describe the experiment. Assuming an initial coverage of 0.22 ML and an identical preexponential factor as for the reaction with oxygen islands—i.e., $\nu^d=\nu$ (with the estimated value of $c=0.05$)—a reasonable fit to the experimental data above 180 K (dotted line in Fig. 8) can be obtained with $E_a^d=0.48$ eV. Note that also in this case the temperature scale of the simulated curve is shifted down by 10 K. From the obtained value for $E_a^d$, the calculated rate constant at 300 K for the reaction of disordered oxygen—e.g., for $\theta_O^d=0.05$ ML—would be higher by a factor of approximately 20 compared to the rate of oxygen in islands at $\theta_O=0.17$ ML. Even considering the large error margins possible in the evaluation, always a considerably higher rate constant is found.

## IV. SUMMARY

We have examined the coadsorption and reaction of CO with atomic oxygen on Pt(111) by *in situ* high-resolution core level spectroscopy using synchrotron radiation. A p$(2\times2)$ atomic oxygen layer with a coverage of 0.25 ML was exposed to CO from a supersonic molecular beam at various sample temperatures and pressures. O 1s spectra and in selected cases C 1s spectra have been used to determine the surface coverage of the adsorbed species.

At a temperature of 120 K or below, no reaction takes place between the preadsorbed oxygen and adsorbed CO; in accordance with the literature, bridge sites are blocked for CO adsorption in the presence of the O-p$(2\times2)$ adlayer. For

CO on-top sites, a saturation coverage of $(0.23\pm0.02)$ ML is observed at 160 L. Compared to CO on clean Pt(111), this implies that also part of the on-top sites is blocked by the presence of atomic oxygen. This finding stands in contrast to the TPD results of Kostov *et al.*,[13] where after 100 L already a CO coverage of 0.41 ML on the O-p$(2\times2)$ adlayer is reported. The origin of this discrepancy remains unclear.

The kinetics of the reaction were examined for sample temperatures between 275 and 305 K. Immediately after the start of the CO exposure at high pressure ($1.3\times10^{-6}$ mbar), a sudden drop of the oxygen coverage and, simultaneously, a fast increase of CO on bridge sites have been observed, with both changes amounting to 0.03–0.06 ML. This process is attributed to the reaction of CO with disordered oxygen atoms, which at the temperatures studied has a higher reaction rate than the reaction of CO with ordered p$(2\times2)$ oxygen islands. The disordered areas, which are present although a sharp p$(2\times2)$ LEED pattern is observed, act as a starting point of the reaction.

By investigating the reaction behavior for different pressures, it was found that around 300 K the reaction rate saturates for CO pressures higher than $\sim9\times10^{-7}$ mbar, while it decreases if the pressure is reduced. From the data collected under different experimental conditions, a reaction of the adsorbed CO molecules within the ordered oxygen p$(2\times2)$ islands—i.e., a first-order reaction kinetics—can be excluded. From our measurements for sufficiently high pressure (where the rate is independent of pressure), we obtain a reaction order $\alpha$ with respect to oxygen of $0.63\pm0.15$. This value is in good agreement with a previous STM study by Wintterlin *et al.*[7] at somewhat lower temperatures and can be explained if the reaction between O and CO is restricted to the edges of extended ordered oxygen p$(2\times2)$ islands—in that case one would expect an ideal value of $\alpha=0.5$. From an Arrhenius plot of the rate constant between 275 and 305 K, an activation energy of $(0.53\pm0.04)$ eV and a prefactor of $4.7\times10^{6\pm0.7}$ $s^{-1}$ are determined. These values are again in good agreement with the results of Wintterlin *et al.*[7]

The obtained parameters were checked by following the reaction in a temperature-programmed way and comparing the calculated change of oxygen coverage with the data points. If, additionally to the reaction rate of oxygen islands, a rate law for the reaction of disordered regions of oxygen is taken into account, the simulation leads to a good description of the experiment. This supports the evidence of a higher reaction rate of disordered oxygen as compared to compact islands.

## ACKNOWLEDGMENTS

This work was supported by the Deutsche Forschungsgemeinschaft through Grant No. STE 620/4-2. We would like to thank the BESSY staff for technical support.

[1] R. L. Palmer and J. N. Smith, J. Chem. Phys. **60**, 1453 (1974).
[2] T. Engel and G. Ertl, Adv. Catal. **28**, 1 (1979).
[3] T. Matshushima, D. B. Almy, and J. M. White, Surf. Sci. **67**, 89 (1977).
[4] J. L. Gland and E. B. Kollin, J. Chem. Phys. **78**, 963 (1983).
[5] M. D. Xu, J. Y. Liu, and F. Zaera, J. Chem. Phys. **104**, 8825 (1996).
[6] F. Zaera, J. Y. Liu, and M. D. Xu, J. Chem. Phys. **106**, 4204 (1997).
[7] J. Wintterlin, S. Völkening, T. V. W. Janssens, T. Zambelli, and G. Ertl, Science **278**, 1931 (1997).
[8] S. Völkening and J. Wintterlin, J. Chem. Phys. **114**, 6382 (2001).
[9] D. Kulginov, M. Persson, C. Åkerlund, I. Zoric, and B. Kasemo, J. Vac. Sci. Technol. A **13**, 1511 (1995).
[10] J. L. Gland and E. B. Kollin, Surf. Sci. **151**, 260 (1985).
[11] S. Akhter and J. M. White, Surf. Sci. **171**, 527 (1986).
[12] K. Bleakley and P. Hu, J. Am. Chem. Soc. **121**, 7644 (1999).
[13] K. L. Kostov, P. Jakob, and D. Menzel, Surf. Sci. **377–379**, 802 (1997).
[14] J. Yoshinobu and M. Kawai, J. Chem. Phys. **103**, 3220 (1995).
[15] A. Baraldi, G. Comelli, S. Lizzit, M. Kiskinova, and G. Paolucci, Surf. Sci. Rep. **49**, 169 (2003).
[16] A. Baraldi, S. Lizzit, D. Cocco, G. Comelli, G. Paolucci, M. Kiskinova, and R. Rosei, Surf. Sci. **385**, 376 (1997).
[17] I. Z. Jones, A. Bennet, and M. Bowker, Surf. Sci. **439**, 235 (1999).
[18] R. Denecke, M. Kinne, C. M. Whelan, and H. P. Steinrück, Surf. Rev. Lett. **9**, 797 (2002).
[19] M. Kinne, T. Fuhrmann, C. M. Whelan, J. F. Zhu, J. Pantförder, M. Probst, G. Held, R. Denecke, and H. P. Steinrück, J. Chem. Phys. **117**, 10 852 (2002).
[20] M. Kinne, Ph.D. thesis, Universität Erlangen-Nürnberg, 2004.
[21] S. Kneitz, J. Gemeinhardt, H. Koschel, G. Held, and H. P. Steinrück, Surf. Sci. **435**, 27 (1999).
[22] J. L. Gland, B. A. Sexton, and G. B. Fisher, Surf. Sci. **95**, 587 (1980).
[23] H. Steininger, S. Lehwald, and H. Ibach, Surf. Sci. **123**, 1 (1982).
[24] N. Materer, U. Starke, A. Barbieri, R. Döll, K. Heinz, M. A. Van Hove, and G. A. Somorjai, Surf. Sci. **325**, 207 (1995).
[25] C. Puglia, A. Nilsson, B. Hernnäs, O. Karis, P. Bennich, N. Materer, and N. Mårtensson, Surf. Sci. **342**, 119 (1995).
[26] D. A. Shirley, Phys. Rev. B **5**, 4709 (1972).
[27] S. Doniach and M. Šunjic, J. Phys. **3**, 285 (1970).
[28] H. Froitzheim, H. Hopster, H. Ibach, and S. Lehwald, Appl. Phys. **13**, 147 (1977); I. Zasada and M. A. Van Hove, Surf. Rev. Lett. **7**, 15 (2000); F. Bondino, G. Comelli, F. Esch, A. Locatelli, A. Baraldi, S. Lizzit, G. Paolucci, and R. Rosei, Surf. Sci. **459**, L467 (2000).
[29] O. Björneholm, A. Nilsson, H. Tillborg, P. Bennich, A. Sandell, B. Hernnäs, C. Puglia, and N. Mårtensson, Surf. Sci. **315**, L983 (1994).
[30] T. Engel and G. Ertl, J. Chem. Phys. **69**, 1267 (1978).
[31] A. Eichler, Surf. Sci. **498**, 314 (2002).